Properties of Wire Arc-Sprayed Fe-Based Coatings

Subjects: Metallurgy & Metallurgical Engineering | Engineering, Manufacturing
Contributor: Joseph Ndiithi Ndumia

Among different thermal spraying methods, arc-spraying has been widely used due to its low operating costs and high deposition efficiency. The rapid progress of cored wire technology in arc-spraying has increased possibilities for the preparation of new Fe-based coating materials with enhanced properties by adding reinforcement particles and alloying elements to suit the different applications.

Keywords: wire arc-spraying ; Fe-based coatings ; corrosion ; wear ; high-temperature resistance

1. Working Principle of the Arc-Spraying Process

The arc-spraying process melts wires with an electric arc formed at the tip, and the molten or semi-molten materials propelled by a stream of high-pressure velocity gas onto a substrate material to form the coating (**Figure 1**) [1]. Air, N_2, and CO_2 are some of the atomizing gases used in the spraying process. The arc-spraying set-up consists of compressed gas supply, wire feed, arc-spray gun, spray controller, and power supply. The coating formed results from the overlapping splats that interlock and build on top of one another with a cooling rate of ~10^5 K/s [2]. Molten particles from the electrode tips can reach a temperature of up to 4000–6000 °C; the particles are accelerated toward the substrate surface by an atomizing gas with pressure in the range of 0.27–0.6 MPa; the velocity of particles <300 m/s. Coatings obtained have high adhesion strength of approximately 28–41 MPa and porosity levels of around 3–10%, but this has been improved over time by the formation of amorphous/nanocrystalline coatings and addition of reinforcement particles as shown in **Table 1** and **Table 2** [1]. In comparison with arc-spraying, high-velocity arc-spraying (HVAS) provides the molten particles with a higher atomizing air pressure and velocity, which improves the quality of the coatings [3][4].
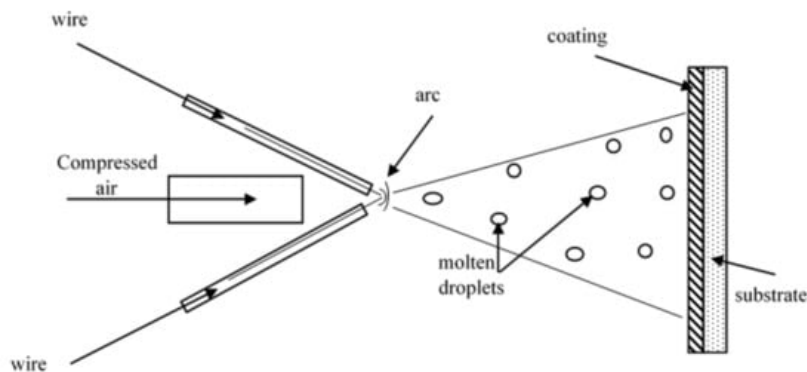

Figure 1. Illustration of the arc-spraying process.

Table 1. Comparison of properties for arc-sprayed Ni-based and Fe-based coatings.

Fe-Based Coatings	Coating Properties			References
	Hardness	Porosity	Bond Strength	
FeTi/CrB	62.7 HRC (~805 HV)	2.7%	40.21 MPa	[5]
FeCrB	811.4 $HV_{0.1}$–920.1 $HV_{0.1}$	3.31%–4.01%	-	[6]
FeNiBCrSi	700–1025 $HV_{0.1}$	-	57 MPa	[7]
FeCrBSiNbW	14.7 GPa (~1499 HV)	2.8%	-	[8]
FeNiCrBSiNbW	850–1000 $HV_{0.1}$	1.8%	52.1 MPa	[9][10]
FeCrNiNbBSiMo	-	3.46%	42.3 MPa	[11]

	Hardness	Porosity	Bond Strength	References
FeAl	6.47 GPa (~659.7 HV)	1.83%	24.5 MPa	[12]
FeNiB-Cr$_3$C$_2$	1090 HV$_{0.1}$	2.1%	-	[13]
FeCrB-Cr$_3$C$_2$	860–1260 HV$_{0.1}$	2.33%	-	[14]
FeCr	480 HV$_{0.1}$	5.02%	-	[15]
FeCrSiB	650 HV$_{0.1}$	4.08%	-	[15]
FeNiCrAl	626 HV$_{0.1}$	8.76%	52.3 MPa	[16]
3Cr13/FeNiCrAl	375–390 HV$_{0.1}$	-	45.7 MPa	[17]
Fe-Cr-B-C	6.47 GPa (~659.7 HV)		-	
Ni-Based Coatings	**Coating Properties**			
	Hardness	Porosity	Bond Strength	References
FeCrAl/Ni95Al	530 HV$_{0.1}$	-	43 MPa	[18]
NiCrMoAl	3.65 ± 0.56 GPa (~372.2 HV)	2.4%	-	[19]
Ni-5Al	290 HV	<2%		[20]
Ni-5Al	203.8 HV & 249 HV	1.55%–1.58%	-	[21]
Ni-20Cr	273.5 HV & 379.8 HV	1.53%–1.54%	-	[21]
NiCrTi	380 HV$_{0.1}$	2.49%	-	[15]
Ni-30Cr	244 ± 12 HV$_{0.3}$	8.4%		
Ni-45Cr	242 ± 11 HV$_{0.3}$	5.0%	-	[22]
Ni-50Cr	209 ± 7 HV$_{0.3}$	6.1%		

Table 2. Summary of the wear and mechanical properties of the arc-sprayed Fe-based coatings.

Coating	Porosity	Hardness (H)	Elastic Modulus (GPa)	H/E	Specific Wear Rate	Wear Mechanism
FeCrBSiNbW	2.8%	14.7 GPa (~1499) HV	198	0.074	-	Dispersion strengthening of the amorphous/nanocrystalline grains prevent the material removal [8]
Fe-NiB Fe-NiB-Cr$_3$C$_2$	2.7% 2.1%	950 HV$_{0.1}$ 1090 HV$_{0.1}$	-	-	-	Wear mechanism of the coatings was by flaking off and some slight plastic furrows [13]
Fe-CrB-Cr$_3$C$_2$	2.33%	860–1260 HV$_{0.1}$	-	-	-	High hardness prevented micro-cutting. Mass loss by flaking mechanism [14]
FeBSiNb	1.2%	16.42 GPa (~1674) HV	219	0.075		Brittle failure and fracture [23]
FeBSiCrNbMnY	1.7%	15.7 GPa (900–1050) HV$_{0.1}$	217	0.07	-	Brittle failure and fracture [24][25]
3Cr13		6.9 GPa (~704) HV	199	0.035	-	Big pits and parallel grooves characterize cutting and delamination [26]
FePSiBNb	<3%	12.3 GPa (~1254) HV	204	0.06	$(0.57 - 1.86) \times 10^{-5}$ mm^3/Nm (at different loads and sliding speeds)	Oxidative wear coupled with delamination [26]

Coating	Porosity	Hardness (H)	Elastic Modulus (GPa)	H/E	Specific Wear Rate	Wear Mechanism
Fe-FeB-WC/12Co Fe-FeB-WC/12Ni	2.1% 3.2%	920 $HV_{0.1}$ 872 $HV_{0.1}$	-	-	-	Selective removal of the binder caused by plastic deformation and fatigue [27]
FeCrCMoBWSiNb (140MXC)	1.55%	9.1 GPa (~928) HV	-		-	Delamination in combination with plastic deformation and oxidation [28]
FeNiCrBCSi	2.1%	960 $HV_{0.3}$	-	-	-	Selective removal of the binder is probably caused by the plastic deformation and fatigue, Flaking off caused by microcracks [29]
08Mn2Si 4Cr13 65Mn	6.12% 3.33% 5.43%	231.2 HV 288.9 HV 329.9 HV	-	-	-	Abrasive wear [30]
FeCrMnMoWBCSi	4.85%	883.8 $HV_{0.1}$			-	Fatigue wear and oxidation wear [31]
FeCrBSiMnMoW	2.53%	1150 $HV_{0.3}$	-	-	3.3×10^{-5} mm^3/Nm	Abrasive wear mechanism with brittle peeling pit and cracks [32]
FeNiCrAlBRE/Ni95Al	3.74 %	480–600 $HV_{0.1}$	-	-	-	Fracture of splats due to severe plastic deformation at the tip of splats. Cracks initiated at the edges of pores, between the boundaries of inclusions and splats or interfaces of splats [33]
FeNiCrAl/3Cr13	-	375–390 $HV_{0.1}$	-	-	1.963 mm^3/Nm	Abrasive wear mechanism [17]
WC/W2C-FeCMnSi	5.4% 4.4% 2.7% 2.9% 3.3%	567 ± 63 $HV_{0.3}$ 543 ± 86 $HV_{0.3}$ 561 ± 79 $HV_{0.3}$ 585 ± 117 $HV_{0.3}$ 630 ± 65 $HV_{0.3}$	84.0 81.9 118.3 124.8 151.4	0.057 0.055 0.051 0.042 0.051	-	[34]
FeBSiNbCrMo	1.1%	18.7 GPa (~1907) HV	-	-	-	Brittle delamination [35]
FeBSiNbCr	1.5%	1113 HV	-	-	-	Brittle breaking and fracture [36]

1.1. Coating Material Preparation

The arc-spraying process uses alloy metal wires and cored wires to prepare coatings. Coatings prepared by alloy metallic materials include: CuAl, ZnAl, AlMg, and NiAl. However, alloy wires are limited due to the few ductile materials and the high hardening tendency of metal alloys during the drawing process. Cored wires contain powdered particles inside a sheath of ductile metal or alloy as illustrated in **Figure 2**. They are beneficial because of their lower cost, shorter production cycle, and combined benefits of the metals and powder materials. They provide diverse options for arc-spraying materials. High hardness materials (oxides, carbides, and nitrides) added into the metal sheath improves the wear and high-temperature resistance of the coatings. The filling factor coefficient, which is the ratio of the core weight to the total weight of the core, determines the material amount in the core. Depending on the diameter of wire, density of core material, and purpose, the filling factor ranges between 15 and 40% [37].
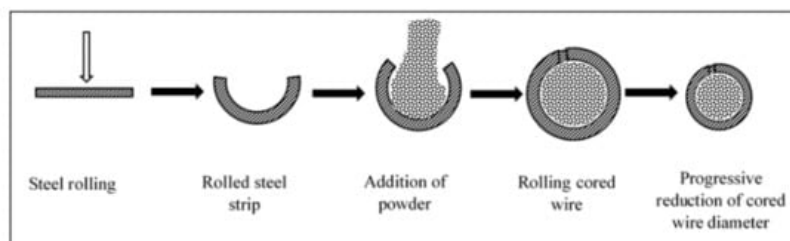

Figure 2. Schematic diagram of cored wire preparation. Reprinted with permission from ref. [38]. Copyright 2007 Elsevier.

1.2. Arc-Sprayed Coating Microstructure

Upon impact on the substrate, molten droplets flatten and solidify to form splats that accumulate and build up the coating. These coatings are characterized by a lamellar structure with alternating layers (**Figure 3**). Studies have shown the correlation between the operating spray parameters (spray distance, current, arc voltage, and atomizing gas pressure) and the microstructural and mechanical properties of arc-sprayed coatings, hence the need for optimization of spray parameters [34][39][40][41][42]. Pores, oxide inclusions, unmelted particles, and cracks may also be present due to some coating imperfections. A high porosity and oxide content reduce the quality of the coatings. As discussed by Li et al. [30], pores in the coating can be generated as a result of the following: air traps in the molten particles during the solidification process; some splats form zonal fractures along the boundaries because of incomplete accumulation of the flat particles; and, during the solidification of the molten droplets, the density difference between the solid and liquid phases of the droplets leads to volumetric shrinkage. Pores can be beneficial to the coating structure because they reduce the friction during the oil wear test by acting as storage structures for oil. The pores, however, should be kept as minimal as possible. In corrosive environments, pores link the corrosion media to the coating, damaging the underlying coating and substrate. Porosity can be effectively reduced by post-coating techniques such as sealing, heat treatment, and laser remelting [39][29]. Oxides found in the coating have been explained as occurring in three different ways [43]: the primary droplets are oxidized during the atomization process as in-flight particles; the secondary droplets are oxidized from splashing; and the coating surface is oxidized after deposition. In some cases, oxides can be beneficial to the coating properties. As stated by Xu et al. [44], the small oxide particles in the $FeAl/Cr_3C_2$ coating structure enhanced the abrasion resistance, erosion resistance, and bonding strength.
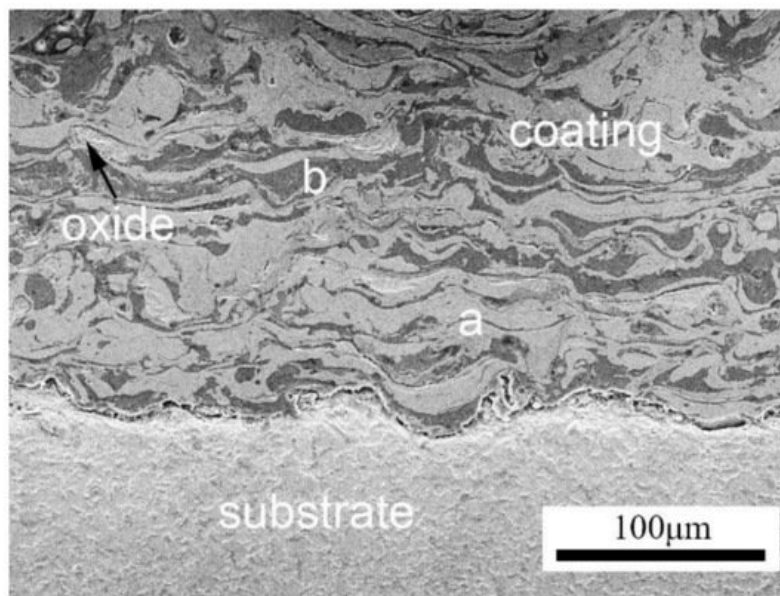

Figure 3. HVAS FeCrAl/Al coating microstructure: (**a**) FeCrAl splats and (**b**) Al splats. Reprinted with permission from ref. [45].

2. Properties of Arc-Sprayed Fe-Based Coatings

2.1. Wear Properties at Room Temperature

Table 2 summarizes the wear properties of some Fe-based coatings.

Post-treatment coating techniques such as annealing, surface remelting, and sealing improve the wear resistance of Fe-based coatings. FeNiCrAl coatings were surface-remelted by the tungsten inert gas welding. The wear resistance improved as a result of the reduced pores and cracks. The main abrasive mechanism was cutting and ploughing [46].

Transition layers or bond coat layers improve the thermal shock resistance and wear resistance by enhancing the bonding strength [47]. FeNiCrAlBRE/Ni95Al was arc-sprayed with Ni95Al applied as a transition layer to improve the adhesive strength between the coating and substrate. The coating had better wear resistance because of the low debris and shallow grooves [33]. Tian et al. [17] reported the abrasive wear properties of the 3Cr13 coating when FeNiCrAl was applied as a transition layer between the coating and the substrate. The low wear volume loss of the composite coating was due to its high hardness caused by evenly distributed $Cr_{23}C_6$ and (Fe, Cr) phase. The hardness-wear resistance relation could be explained by Archard's Equation [48], as shown in Equation (1):

$$V_W = K \times \frac{SN}{H}$$

where V_W is the worn volume, K is the wear coefficient, S is the sliding wear distance, N is the applied load, and H is the hardness.

According to Equation (1), it can be stated that the high coating hardness contributes to the good wear properties. The wear rate of the coating is proportional to the applied load and sliding distance (sliding time and sliding linear speed) [49]. Volume wear losses of the AISI 45 steel substrate and the metallic glass coatings increased linearly with sliding distance (**Figure 4**).
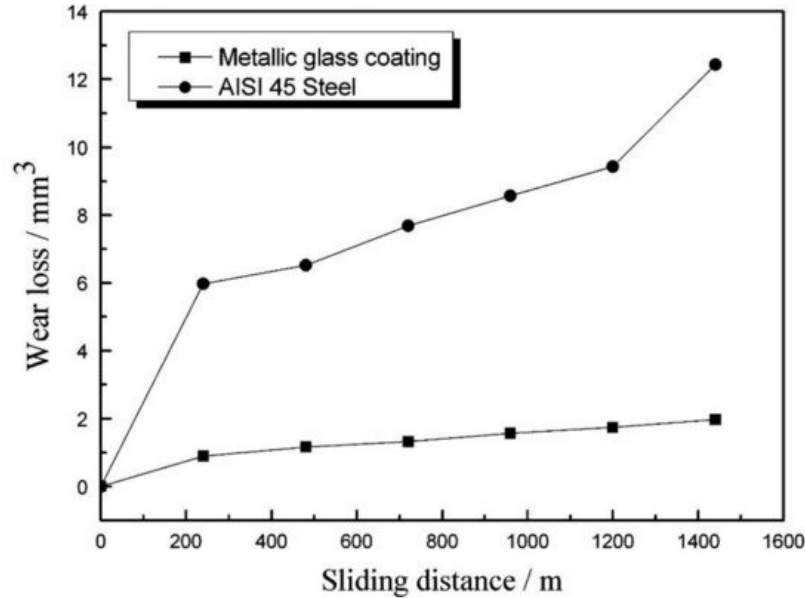

Figure 4. Wear losses of coating and substrate as a function of sliding distance. Reprinted with permission from ref. [50]. Copyright 2013 Elsevier.

It is increasingly being recognized that hardness is not the only primary requirement for wear resistance. Researchers have recently examined the effects of elastic modulus on the wear resistance properties. The induced residual stress and mechanical strength of the coating depend on the elastic modulus. The low elastic modulus and high coating hardness contribute to high wear resistance and elastic energy absorption ability [51]. The microhardness and elastic modulus relationship can be derived from the load-displacement curves data by nanoindentation measurement. The ultra-high strength of the amorphous structure and excellent bonding between the elements improves the coating hardness. H/E shows the depth of penetration that a coating material tolerates without exceeding the elastic limit. A high hardness to elastic modulus H/E ratio indicates good wear resistance of the arc-sprayed coatings. A high H^3/E^2 indicates the resistance of the loaded material to plastic deformation and therefore shows that the material has high toughness [52][53]. **Figure 5** shows a relationship of the hardness elastic modulus for the Q235 steel and three metallic glass coatings. The H/E and H^3/E^2 increased after addition of Cr and Mo elements promoting lower friction and higher wear resistance [35]. The higher value of H/E and H^3/E^2 shows that the ability to absorb applied deformation is strong without exceeding the elastic limit, or adapting to the deformation with less damage [26].
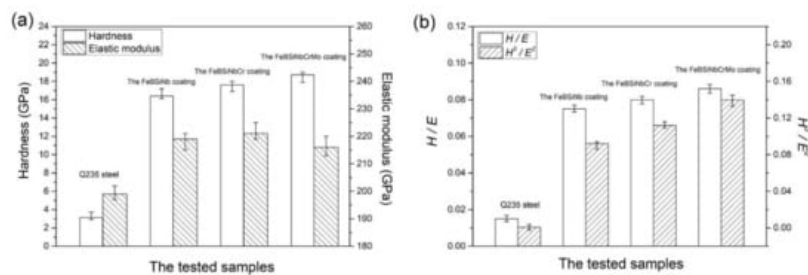

Figure 5. (**a**) Hardness H and elastic modulus E, (**b**) H/E and H^3/E^2 of the samples. Reprinted with permission from ref. [35]. Copyright 2018 Elsevier.

In summary, the wear properties of the Fe-based coatings depend on the coating microstructure, the additional hard reinforcement particles, and the mechanical properties, including hardness and elastic properties. Similarly, the amorphous/nanocrystalline phase structure of the coatings improves wear resistance as a result of the dispersion

strengthening effect caused by the homogenous amorphous phase in the glassy state. Further research should be conducted to improve the tribological properties of arc-sprayed Fe-based amorphous coatings by adding reinforcement particles such as WC, Cr_3C_2, and Al_2O_3.

2.2. Corrosion Properties at Room Temperature

Corrosion is among the leading causes of degradation of materials, especially equipment and structures exposed to marine environments. Coating defects such as pores and cracks have adverse impacts on the corrosion properties. They act as passages for the corrosive media, and they should be minimized in the coating microstructure.

The coating microstructure needs to be free of defects such as pores, oxides, unmelted particles, and cracks that accelerate the passage of electrolytes into the underlying coating. Oxides formed during the spraying process also degrade the corrosion resistance by reducing the adhesive strength between the coating splats. These defects can be minimized by optimizing the arc-spraying parameters. Crystallization of amorphous coatings during annealing causes lattice mismatch and strain, which weakens the coherence between the oxide films and metal, leading to the rupture of oxide films [54]. Thus, the annealing temperature and time should be controlled to obtain the optimum properties. Although some research has been carried out on the corrosion behavior of annealed Fe-based amorphous coatings, there is very little discussion about the corrosion behavior of annealed Fe-based crystalline alloys.

2.3. High-Temperature Properties of Arc-Sprayed Fe-Based Coatings

2.3.1. High-Temperature Oxidation Behavior

Li et al. [55] studied the oxidation properties of FeCrB(CSi) coatings with different chromium concentrations. The increase in the Cr content (17, 21, 25 at. %) improved the high-temperature oxidation resistance due to the formation of a protective Cr_2O_3 oxide layer that inhibited further oxygen penetration. The coating with the highest amount of Cr (25 at. %) had the least weight gain compared with the uncoated steel substrate and commercial FeCrAl coating. Boron and silicon elements controlled the oxidation of molten particles, thereby preventing Cr consumption. Li et al. [56] also investigated the influence of Cr content (15, 20, 25, 30, 35, 40 at. %) on the high-temperature oxidation properties of Fe-Cr and compared with Ni-Cr-Ti coatings to determine the suitability of Fe-based coatings as substitutes for Ni-based coatings. The Fe-Cr coatings had better high-temperature oxidation resistance than the SA213-T2 substrate used in boiler tubes. The thickness of the oxide scales and final weight gain of the Fe-Cr coatings decreased with an increase in the Cr content at 650 °C for 2 h. The Fe-35Cr and Fe-40Cr had the lowest weight gain rates, showing excellent high-temperature oxidation resistance because of the Cr_2O_3 and Fe_2O_3 oxide scales that protected the underlying substrate. The high-temperature oxidation resistance of the Fe-35Cr and Fe-40Cr coatings was close to that of the Ni-Cr-Ti coatings.

Oxidation tests conducted by Wielage et al. [57] and Vasyl et al. [58] explained the different morphology of oxides formed according to the chemical composition of individual lamellae. **Figure 6** shows the oxide films that formed on different lamellae of the arc-sprayed coating [57][58]. The needle-shaped Fe_2O_3 formed on the lamellae with low Al and Cr content, monolithic clusters of chromium oxide or alloyed hematite $(Fe, Cr)_2O_3$ formed on the lamellae with higher Cr content, while a dense flat oxide film $(Fe, Al)_2O_3$ formed on the Al-rich lamellae. According to [59], the Fe-based coatings also formed distinctive morphologies depending on their chemical composition. At 800 °C, dense oxide films formed and with increase in temperature to 900 °C, the pores and cracks were filled by a netted oxide scale, which effectively protected the substrate during the long-term exposure.
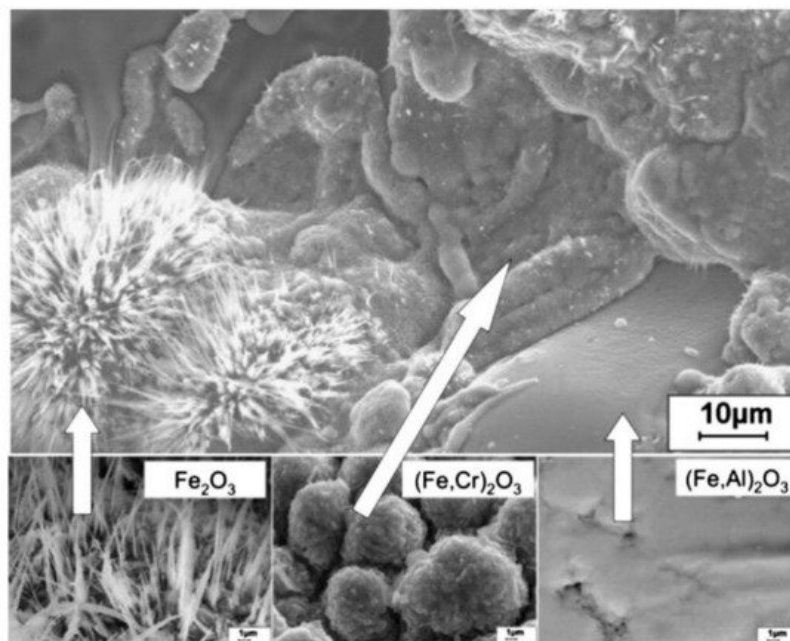
Figure 6. Different morphology of the oxide scales formed on the various lamellae of arc-sprayed coating Cr6B3Al4. Reprinted with permission from ref. [57]. Copyright 2013 Elsevier.

In conclusion, the high-temperature oxidation of the Fe-based coatings depends on the formation of oxide scales that protect the coatings from further oxidation. Suitable alloying elements such as Cr and Al should be selected and their compositions optimized to enhance the high-temperature oxidation resistance.

2.3.2. High-Temperature Erosion (HTE) Behavior

High-temperature erosion (HTE) has led to the deterioration of turbines, and fluidized bed combustion boilers exposed to particulates flow and fly ash particles. Different factors such as impact angle, impingement velocity, and temperature affect erosion resistance of thermally sprayed coatings. Luo et al. [60] investigated the effects of Al content (0, 8, 15 at. %) on the erosion properties of the FeMnCrAl/Cr_3C_2 coating. Sample coatings with 15% Al had the best HTE resistance because of the finer microstructure with low oxide inclusions and pores. The coating without Al had the highest erosion rate under particle impacting. The high amount of oxide fractions weakened the bonding of splats and propagated cracks leading to brittle breaking and lamellar spalling. This study provides a major contribution in the advancement of knowledge on the effects of elemental composition on HTE behavior. Narrow grain size distribution of powders can be applied in arc-spraying cored wires to improve the erosion resistance as used in HVOF thermally sprayed WC-Co-Cr coatings. Narrow powder grain size distribution (36–45 µm) coating gave a higher erosion-corrosion resistance than wider grain size distribution (15–45 µm) because of the different melting behaviors. Overheating of small grains produced phases with lower erosion resistance, hence poor coating quality, while large grains were insufficiently heated, leading to a more porous coating [61]. Nanoparticle coatings produced have higher hardness and toughness as a result of the low porosity and coating defects, which can significantly affect the erosion resistance properties.

2.3.3. High-Temperature Corrosion Behavior

Hot corrosion generally refers to the accelerated oxidation of metals and alloys at intermediate temperatures (600–850 °C) associated with mixed molten salts (e.g., sulphates deposited by alkali metals). Few studies on the high-temperature corrosion properties have been reported and further research on the effect of elemental compositions could be undertaken. Shukla et al. [62] fabricated arc-sprayed FeCrBSiMn coating with superior high-temperature corrosion resistance exposed to a molten salt environment (Na_2SO_4 − 82%$Fe_2(SO_4)_3$) at 900 °C under cyclic conditions for 50 cycles. They noted that the oxides of Fe and Cr enhanced the corrosion resistance of the coatings. Xu et al. [44] prepared HVAS Fe-Al/Cr_3C_2 coatings on 20-grade steel. The coatings had a lower corrosion rate than the substrate. The Fe-Al matrix composites and Cr_2C_3 had good corrosion properties and the oxides formed protected the coatings. The corrosion rate increased with temperature but later slowed down with increased time. Cr_2O_3 facilitated the formation of Al_2O_3 that further protected the coating. Guo et al. [63] studied the hot corrosion resistance of FeCrBC in a mixed solution of Na_2SO_4 + K_2SO_4 (7:3) at 700 °C for 156 h. Thin films of Cr_2O_3 formed on the coating and separated the alloy from the mixed salt solution, thus providing better resistance to hot corrosion. In a comparison study by Li et al. [15], the arc-sprayed FeCrSiB coatings provided better hot corrosion resistance than FeCr, approaching that of NiCrTi coating. The weight gain for the hot corrosion has been calculated as follows:

$$\Delta W_i = \left[\frac{W_{i+2} - W_i}{A}\right] - \left[\frac{W_{i+1} - W_i}{A}\right] \times 0.6$$

where, W_i is the mass of the sample before the ith corrosion, W_{i+1} is the mass after the first salt coating, W_{i+2} is the mass after the ith corrosion, A is the total surface area of the sample, and 0.6 is the coefficient for deducting the salt film crystal water.

2.3.4. High-Temperature Wear Behavior

Several studies have shown the relation between the coating integrity and the coating's high-temperature wear performance. Stress concentration occurs at the defects such as cracks on the coating, which propagate coating failure during the wear process [64]. The coating hardness, cohesive strength of the coating, and bond strength of the coating with substrate influence the high-temperature wear properties.

The phase composition of the coatings and the oxides formation controlled the high-temperature wear, oxidation, corrosion, and erosion resistance. The oxide scales generated stresses that determined the spalling and cracking of the coatings. Adding alloying elements such as Al and Cr is vital to form oxides that reduce the wear and corrosion rate at high temperatures. The coating defects undermine the coating protection at high temperatures, hence the need to minimize them through process optimization. The high-temperature wear resistance has mostly been characterized by the weight gain and weight reduction of the coatings. The degradation of coatings in corrosive medium at high temperature involves the combination of wear process and the electrochemical corrosion process. The corrosion-wear behavior of arc-sprayed Fe-based coatings should be investigated at high temperatures to further understand the tribological properties.

3. Conclusions and Future Scope Recommendations

Arc-spraying is a reliable and effective technique used in the production of Fe-based coatings. Arc-sprayed Fe-based coatings are recommended for application in boilers, steam pipes, and components operating at high temperatures due to the high resistance offered with respect to oxidation, corrosion, wear, and erosion. Fe-based coatings have potential to be used as alternatives to some of the Ni-based coatings because of their relatively lower costs and availability of raw materials. Some Ni-based coatings produce oxidation products such as NiO and $NiCl_2$, which may be harmful to human health [56]. The protective mechanisms of Fe-based coatings were discussed and the following conclusions and recommendations are made:

- The density, size, and structure of feedstock powders influence the phase composition of the deposited coatings in HVOF and APS thermal spraying methods. Cored wires in arc-spraying can explore the use of different-sized powders as filling materials to optimize the coating properties. Coating powders of arc-sprayed cored wires can apply nanoscale particles that result in densely packed nanostructured coatings [65]. Arc-sprayed FePSiNb coatings exhibited a nanoscale structure with a grain size range from 12 to 50 nm with good wear resistance properties [26]. More work will need to be done to determine the production and study of properties of arc-sprayed nanostructured coatings.

- The spraying parameters play an important role in determining the microstructural properties of the coatings. Optimizing methods such as response surface methodology (RSM) analyzes the interaction between spray parameters and their influence on the coating properties. The effects of process parameters on the amorphization of the arc-sprayed coatings could be studied to maximize the amorphous content of Fe-based amorphous coatings.

- The arc-sprayed Fe-based coatings have better hardness and wear resistance properties than conventional alloys due to the dense microstructure, the dispersion strengthening of the amorphous/nanocrystalline phases, and reinforcement ceramic particles. The elastic properties also determine the wear resistance of the Fe-based coatings.

- To increase the corrosion resistance, the coating defects (oxides, pores, and cracks) in the Fe-based coatings should be minimized by optimizing spray parameters to prevent the deterioration of coating properties in corrosive media.

- The high-temperature properties of the Fe-based coating are mainly affected by the microstructure and the elemental composition. The reinforcement ceramic particles added to the Fe-based alloys improve the tribological and high-temperature coating performance while the amorphous phase content is characterized by fewer dislocations, microcracks, and grain boundaries enhancing the properties of the Fe-based amorphous coatings. Future research should focus on understanding the combined corrosion-wear behavior of arc-sprayed Fe-based coatings at elevated temperatures.

- Adding appropriate alloying elements such as Al and Cr to Fe-based coatings improves high-temperature protection by forming oxide scales that prevent further oxidation of the underlying substrate. Future research should investigate the influence of different elements on high-temperature properties of Fe-based coatings.

References

1. Talib, R.; Saad, S.; Toff, M.; Hashim, H. Thermal spray coating technology: A review. Solid State Sci Technol. 2003, 11, 109–117.

2. Takalapally, S.; Kumar, S.; Pusuluri, S.H.; Palle, M. A critical review on surface coatings for engineering materials. Int. J. Mech. Eng. Technol. 2016, 7, 80–85.

3. Liu, G.; Rożniatowski, K.; Kurzydłowski, K. Quantitative characteristics of FeCrAl films deposited by arc and high-velocity arc spraying. Mater. Charact. 2001, 46, 99–104.

4. Zhan, J.; Li, Z.; Lu, J.; Wu, Y.; Zhao, L.; Yu, N. Technics and performance analysis of Monel alloy coating prepared by high velocity arc spraying. Mater. Res. Innov. 2013, 17, 112–114.

5. Wang, Y.; Sun, C.; Sun, J.; Zhao, W.; Dong, L.; Li, L.; Meng, F. Erosion behavior of arc sprayed FeTi/CrB MMC coating at elevated temperature. Surf. Coat. Technol. 2015, 262, 141–147.

6. Yao, H.; Zhou, Z.; Wang, Y.; He, D.; Bobzin, K.; Zhao, L.; Öte, M.; Königstein, T. Microstructure and properties of FeCrB alloy coatings prepared by wire-arc spraying. J. Therm. Spray Technol. 2017, 26, 483–491.

7. He, D. Study on arc-sprayed cored wires and wear properties of coatings. Ph.D Thesis, Beijing University of Technology, Beijing, China, 2004.

8. Cheng, J.; Wang, Z.; Xu, B. Wear and corrosion behaviors of FeCrBSiNbW amorphous/nanocrystalline coating prepared by arc spraying process. J. Therm. Spray Technol. 2012, 21, 1025–1031.

9. Lin, J.; Wang, Z.; Lin, P.; Cheng, J.; Zhang, J.; Zhang, X. Microstructure and corrosion resistance of Fe-based coatings prepared by twin wires arc spraying process. J. Therm. Spray Technol. 2014, 23, 333–339.

10. Lin, J.; Wang, Z.; Lin, P.; Cheng, J.; Zhang, X.; Hong, S. Microstructure and cavitation erosion behavior of FeNiCrBSiNbW coating prepared by twin wires arc spraying process. Surf. Coat. Technol. 2014, 240, 432–436.

11. Zhang, X.; Wang, Z.; Lin, J.; Zhou, Z. A study on high temperature oxidation behavior of high-velocity arc sprayed Fe-based coatings. Surf. Coat. Technol. 2015, 283, 255–261.

12. Xu, B.; Zhu, Z.; Ma, S.; Zhang, W.; Liu, W. Sliding wear behavior of Fe–Al and Fe–Al/WC coatings prepared by high velocity arc spraying. Wear 2004, 257, 1089–1095.

13. Fu, B.-Y.; He, D.-Y.; Zhao, L.-D.; Li, X.-Y. Microstructure characterisation and wear properties of arc sprayed NiB containing amorphous coatings. Surf. Eng. 2009, 25, 326–332.

14. Fu, B.-Y.; He, D.-Y.; Zhao, L.-D.; Jiang, J.-M.; Li, X.-Y. Microstructure and properties of arc sprayed coatings containing Fe based amorphous phase and nanocrystallites. Surf. Eng. 2009, 25, 333–337.

15. Li, R.; Zhou, Z.; He, D.; Wang, Y.; Wu, X.; Song, X. Microstructure and high temperature corrosion behavior of wire-arc sprayed FeCrSiB coating. J. Therm. Spray Technol. 2015, 24, 857–864.

16. Tian, H.; Wang, C.; Tang, Z.; Wei, S.; Xu, B.; Que, M. Effect of high velocity arc spraying parameters on properties of FeNiCrAl coating. J. Aeroun. Mater. 2016, 36, 40–47.

17. Tian, H.; Wei, S.; Chen, Y.; Tong, H.; Liu, Y.; Xu, B.S. Adhesive strength and abrasive property of Fe based composite coating deposited by high velocity arc spraying. Mater Res Innov. 2014, 18, S2-363–S2-367.

18. Tian, H.; Wei, S.; Chen, Y.; Tong, H.; Lui, Y.; Xu, B. Properties of FeCrAl/Ni95Al coating by high velocity arc spraying. Heat Treat. Metals 2013, 38, 92–96.

19. Daram, P.; Munroe, P.; Banjongprasert, C. Microstructural evolution and nanoindentation of NiCrMoAl alloy coating deposited by arc spraying. Surf. Coat. Technol. 2020, 391, 125565.

20. Kant, S.; Kumar, M.; Chawla, V.; Singh, S. Study of high temperature oxidation behavior of wire arc sprayed coatings. Mater. Today Proc. 2020, 21, 1741–1748.

21. Kumar, S.; Kumar, M.; Handa, A. Comparative study of high temperature oxidation behavior and mechanical properties of wire arc sprayed NiCr and NiAl coatings. Eng. Fail. Anal. 2019, 106, 104173.

22. Cheng, J.; Wu, Y.; Chen, L.; Hong, S.; Qiao, L.; Wei, Z. Hot corrosion behavior and mechanism of high-velocity arc-sprayed Ni-Cr alloy coatings. J. Therm. Spray Technol. 2019, 28, 1263–1274.

23. Cheng, J.; Liang, X.; Wang, Z.; Xu, B. Microstructure and mechanical properties of FeBSiNb metallic glass coatings by twin wire arc spraying. J. Therm. Spray Technol. 2013, 22, 471–477.

24. Cheng, J.-B.; Liang, X.-B.; Xu, B.-S.; Wu, Y.-X. Formation and properties of Fe-based amorphous/nanocrystalline alloy coating prepared by wire arc spraying process. J. Non-Cryst. Solids. 2009, 355, 1673–1678.

25. Cheng, J.; Liang, X.; Xu, B.; Wu, Y. Characterization of mechanical properties of FeCrBSiMnNbY metallic glass coatings. J. Mater. Sci. 2009, 44, 3356–3363.

26. Cheng, J.; Liu, Q.; Sun, B.; Liang, X.; Zhang, B. Structural and tribological characteristics of nanoscale FePSiBNb coatings. J. Therm. Spray Technol. 2017, 26, 530–538.

27. He, D.-Y.; Fu, B.-Y.; Jiang, J.-M.; Li, X.-Y. Microstructure and wear performance of arc sprayed Fe-FeB-WC coatings. J. Therm. Spray. Technol. 2008, 17, 757–761.

28. Arizmendi-Morquecho, A.; Campa-Castilla, A.; Leyva-Porras, C.; Aguilar Martinez, J.A.; Vargas Gutiérrez, G.; Moreno Bello, K.J.; López López, L. Microstructural characterization and wear properties of Fe-based amorphous-crystalline coating deposited by twin wire arc spraying. Adv. Mater. Sci. Eng. 2014, 2014, 836739.

29. Fu, B.-Y.; He, D.-Y.; Zhao, L.-D. Effect of heat treatment on the microstructure and mechanical properties of Fe-based amorphous coatings. J. Alloys Compd. 2009, 480, 422–427.

30. Li, Z.-R.; Li, D.-Y.; Zhang, N.-N.; Huang, H.; Wang, X. Wear mechanism of iron-based alloy coating by arc spraying. J. Iron Steel Res. Int. 2016, 23, 834–841.

31. Yan, Y.; Wei, X.; Jiang, H.; Ying, C.; Shen, J. Research on microstructure and friction and wear properties of Fe-based amorphous alloy coatings prepared by arc spraying. Hot Work Technol. 2018, 47, 117–121.

32. Wu, D.; Fan, Z.S.; Yang, Y. Formation and properties of Fe-based amorphous/nanocrystalline alloy coating prepared by wire arc spraying process. In Materials Science Forum; Trans Tech Publications: Zürich, Switzerland, 2019; pp. 499–505.

33. Tian, H.; Wei, S.; Chen, Y.; Tong, H.; Liu, Y.; Xu, B. Wear behavior of high velocity arc spraying FeNiCrAlBRE/Ni95Al composite coatings. Physics Procedia 2013, 50, 282–287.

34. Tillmann, W.; Hagen, L.; Kokalj, D. Spray characteristics and tribo-mechanical properties of high-velocity arc-sprayed WC-W2C iron-based coatings. J. Therm. Spray Technol. 2017, 26, 1685–1700.

35. Zhang, B.; Cheng, J.; Liang, X. Effects of Cr and Mo additions on formation and mechanical properties of Arc-sprayed FeBSiNb-based glassy coatings. J. Non-Cryst. Solids. 2018, 499, 245–251.

36. Cheng, J.; Liang, X.; Xu, B.; Wu, Y. Microstructure and wear behavior of FeBSiNbCr metallic glass coatings. J. Mater. Sci. Technol. 2009, 25, 687–690.

37. Boronenkov, V.; Korobov, Y. Fundamentals of Arc Spraying; Springer International Publishing: Geneva, Switzerland, 2016; (Physical and Chemical Regularities).

38. Liu, S.-G.; Wu, J.-M.; Zhang, S.-C.; Rong, S.-J.; Li, Z.-Z. High temperature erosion properties of arc-sprayed coatings using various cored wires containing Ti–Al intermetallics. Wear 2007, 262, 555–561.

39. Zeng, Z.-s.; Sakoda, N.; Tajiri, T. Corrosion behavior of wire-arc-sprayed stainless steel coating on mild steel. J. Therm. Spray Technol. 2006, 15, 431–437.

40. Jandin, G.; Liao, H.; Feng, Z.; Coddet, C. Correlations between operating conditions, microstructure and mechanical properties of twin wire arc sprayed steel coatings. Mater. Sci. Eng. A-Struct. Mater. Prop. Microstruct. Process. 2003, 349, 298–305.

41. Horner, A.L.; Hall, A.C.; McCloskey, J.F. The effect of process parameters on twin wire arc spray pattern shape. Coatings 2015, 5, 115–123.

42. Johnston, A.L.; Hall, A.C.; McCloskey, J.F. Effect of process inputs on coating properties in the twin-wire arc zinc process. J. Therm. Spray Technol. 2013, 22, 856–863.

43. Newbery, A.; Grant, P. Oxidation during electric arc spray forming of steel. J. Mater. Process. Technol. 2006, 178, 259–269.

44. Xu, W.-P.; Xu, B.-S.; Zhang, W.; Wu, Y.-X. High temperature behaviors of high velocity arc sprayed Fe-Al/Cr3C2 composite coatings. Int. J. Miner. Metall. Mater. 2005, 12, 340–346.

45. Ndiithi, N.J.; Kang, M.; Zhu, J.; Lin, J.; Nyambura, S.M.; Liu, Y.; Huang, F. Microstructural and corrosion behavior of high velocity arc sprayed FeCrAl/Al composite coating on Q235 steel substrate. Coatings 2019, 9, 542.

46. Tian, H.; Wei, S.; Chen, Y.; Tong, H.; Liu, Y.; Xu, B. Microstructure and wear resistance of an arc-sprayed Fe-based coating after surface remelting treatment. Strength Mater. 2014, 46, 229–234.

47. Peng, Y.; Zhang, C.; Zhou, H.; Liu, L. On the bonding strength in thermally sprayed Fe-based amorphous coatings. Surf. Coat. Technol. 2013, 218, 17–22.

48. Niu, P.-F.; Tian, B.-L. Wear compensation model based on the theory of archard and definite integral method. Math. Probl. Eng. 2018, 2018.

49. Kumar, D.; Murtaza, Q.; Singh, R.C. Sliding wear behavior of aluminum alloy coating prepared by two-wire electric arc spray process. Int. J. Adv. Manuf. Technol. 2016, 85, 237–252.

50. Cheng, J.; Liang, X.; Wang, Z.; Xu, B. Dry sliding friction and wear properties of metallic glass coating and martensite stainless coating. Tribol. Int. 2013, 60, 140–146.

51. Leyland, A.; Matthews, A. Design criteria for wear-resistant nanostructured and glassy-metal coatings. Surf. Coat. Technol. 2004, 177, 317–324.

52. Leyland, A.; Matthews, A. On the significance of the H/E ratio in wear control: A nanocomposite coating approach to optimised tribological behaviour. Wear 2000, 246, 1–11.

53. Chen, X.; Du, Y.; Chung, Y.-W. Commentary on using H/E and H3/E2 as proxies for fracture toughness of hard coatings. Thin Solid Film. 2019, 688, 137265.

54. Yoo, Y.H.; Lee, S.H.; Kim, J.G.; Kim, J.S.; Lee, C. Effect of heat treatment on the corrosion resistance of Ni-based and Cu-based amorphous alloy coatings. J. Alloy Compd. 2008, 461, 304–311.

55. Li, R.; He, D.Y.; Zhou, Z.; Wang, Z.J.; Song, X.Y. Wear and high temperature oxidation behaviour of wire arc sprayed iron based coatings. Surf. Eng. 2014, 30, 784–790.

56. Li, R.; Zhou, Z.; He, D.; Zhao, L.; Song, X. Microstructure and high-temperature oxidation behavior of wire-arc sprayed Fe-based coatings. Surf. Coat. Technol. 2014, 251, 186–190.

57. Wielage, B.; Pokhmurska, H.; Student, M.; Gvozdeckii, V.; Stupnyckyj, T.; Pokhmurskii, V. Iron-based coatings arc-sprayed with cored wires for applications at elevated temperatures. Surf. Coat. Technol. 2013, 220, 27–35.

58. Luo, L.-M.; Luo, J.; Liu, S.-G.; Liu, Y.-l.; Li, J. Microstructure and high temperature oxidation resistance of FeMnCrAl/Cr3C2 coatings deposited by high velocity arc spraying. Trans. Mater. Heat Treat. 2010, 31, 139–142. (In Chinese)

59. Pokhmurskii, V.; Student, M.; Gvozdeckii, V.; Stypnutskyy, T.; Student, O.; Wielage, B.; Pokhmurska, H. Arc-sprayed iron-based coatings for erosion-corrosion protection of boiler tubes at elevated temperatures. J. Therm. Spray Technol. 2013, 22, 808–819.

60. Luo, L.-M.; Liu, S.-G.; Jia, Y.; Juan, L.; Jian, L. Effect of Al content on high temperature erosion properties of arc-sprayed FeMnCrAl/Cr3C2 coatings. Trans. Nonferr. Met. Soc. China. 2010, 20, 201–206.

61. Berget, J.; Rogne, T.; Bardal, E. Erosion–corrosion properties of different WC–Co–Cr coatings deposited by the HVOF process—influence of metallic matrix composition and spray powder size distribution. Surf. Coat. Technol. 2007, 201, 7619–7625.

62. Shukla, V.; Rana, N.; Jayaganthan, R.; Tewari, V. Degradation Studies of Wire arc Sprayed FeCrBSiMn alloy Coating in Molten Salt Environment. Procedia Eng. 2014, 75, 113–117.

63. Wenmin, G.; Yuping, W.; Gaiye, L.; Qian, W.; Zhihua, H.; Sheng, H. Hot corrosion behavior of a high velocity arc-sprayed Fe-Cr-BC coating. Rare Met. Mat. Eng. 2012, 41, 456–459.

64. Li, X.; Dong, T.; Li, G.; Zhou, X.; Zheng, X. Research status and development trend of high temperature wear resistance of thermal spraying coatings. Hot Work. Technol. 2018, 47, 32–36.

65. Basak, A.; Zein Eddine, W.; Celis, J.-P.; Matteazzi, P. Characterisation and tribological investigation on thermally processed nanostructured Fe-based and Cu-based cermet materials. J. Nanosci. Nanotechnol. 2010, 10, 1179–1184.